Computational and Theoretical Chemistry 1090 (2016) 41–46

Contents lists available at ScienceDirect

Computational and Theoretical Chemistry

journal homepage: www.elsevier.com/locate/comptc

Theoretical kinetic study of the reaction of SF_5 radical with F_2, Cl_2 and SF_5

Cristian Buendía-Atencio [a,b], Gilles P. Pieffet [a], Adela E. Croce [c], Carlos J. Cobos [c,*]

[a] Universidad Antonio Nariño, Facultad de Ciencias, Bogotá, Colombia
[b] The University of Queensland, Research Group on Complex Processes in Geo-Systems, School of Civil Engineering, Brisbane, QLD 4072, Australia
[c] Instituto de Investigaciones Fisicoquímicas Teóricas y Aplicadas (INIFTA), Departamento de Química, Facultad de Ciencias Exactas, Universidad Nacional de La Plata, CONICET, Casilla de Correo 16, Sucursal 4, 1900 La Plata, Argentina

ARTICLE INFO

Article history:
Received 20 April 2016
Received in revised form 25 May 2016
Accepted 27 May 2016
Available online 30 May 2016

Keywords:
SF_5 radical
Rate coefficients
Quantum-chemical calculations
Transition state theory calculations
Statistical adiabatic channel model/classical trajectory calculations

ABSTRACT

A kinetic study of the gas phase reaction of the SF_5 radical with the species F_2, Cl_2 and SF_5 has been performed. Quantum chemical calculations employing the DFT methods B3LYP, BMK, MPWB1K, BB1K and M06-2X combined with the 6-311+G(3df) basis set provide the required relevant parts of the potential energy surfaces. Transition state theory calculations for the $SF_5 + F_2 \rightarrow SF_6 + F$ reaction lead to the rate coefficient $1.4 \times 10^{-12} \exp(-4.1 \text{ kcal mol}^{-1}/RT) \text{ cm}^3 \text{ molecule}^{-1} \text{ s}^{-1}$ at 213–245 K. From similar calculations, the expression $2.1 \times 10^{-11} \exp(-7.6 \text{ kcal mol}^{-1}/RT) \text{ cm}^3 \text{ molecule}^{-1} \text{ s}^{-1}$ was obtained for $SF_5 + Cl_2 \rightarrow SF_5Cl + Cl$. The combination of the rate coefficients obtained for the F atom abstraction reaction with reported experimental kinetic information yields the value $3 \times 10^{-12} \text{ cm}^3 \text{ molecule}^{-1} \text{ s}^{-1}$ for the $SF_5 + SF_5 \rightarrow S_2F_{10}$ association reaction. A comparison with SACM/CT calculations and previous conflicting rate coefficients for this process is presented.

1. Introduction

Sulfur hexafluoride SF_6 is a gas that presents unique features, such as high thermal stability, high dielectric strength and low toxicity, and, as a consequence, has been widely employed in a variety of technological processes [1–4]. Even though at normal operating conditions the SF_6 is thermally and photochemically stable, may explode when subject to an electrical discharge, such as an electrical arc, spark or corona. In the presence of small quantities of water, different byproducts such as HF, SO_2, SOF_2, SO_2F_2, SOF_4, S_2F_{10} are formed [5,6]. The presence of the SF_5 dimer, S_2F_{10}, indicates that the SF_5 radical is probably an intermediate species of the reaction mechanism. This radical has aroused great interest in the environmental area because it may associate with the CF_3 radical or react with fluorinated polymers to generate the extremely potent greenhouse gas SF_5CF_3 [7].

The participation of SF_5 in a number of reaction mechanisms has been proposed. By instance, in the thermal decompositions of F_5SOOSF_5 [8] and $F_5SOOOSF_5$ [9,10], in the CO oxidation by O_2 sensitized by SF_5O radicals [11], in the thermal reaction between SF_4 and F_2 in the presence of O_2 [12] and in the photochemical reaction of F_2O in the presence of SF_4 [13] the SF_5 radical plays an important role as intermediary.

The present investigation is focused on the study of the photolysis of F_2 at 365 nm in the presence of SF_4 at 213–244 K by Aramendía and Schumacher [14]. The main product observed was SF_6 and small amounts of S_2F_{10} with a very significant participation of SF_5 radical. The experimental results were interpreted by the reaction mechanism:

$$F_2 + h\nu_{365\text{ nm}} \rightarrow 2F \quad (1)$$

$$SF_4 + F_2 \rightarrow SF_5 + F \quad (2)$$

$$SF_4 + F \rightarrow SF_5 \quad (3)$$

$$SF_5 + F_2 \rightarrow SF_6 + F \quad (4)$$

$$SF_5 + SF_5 \rightarrow S_2F_{10} \quad (5)$$

$$SF_5 + F \rightarrow SF_6 \quad (6)$$

$$F + F + M \rightarrow F_2 + M \quad (7)$$

The ratio between the rate coefficients of reactions (4) and (5) of $k_4/k_5^{1/2} = 10^{4.18\pm0.01} \exp(-4.0 \pm 0.2 \text{ kcal mol}^{-1}/RT) \text{ M}^{-1/2} \text{ s}^{-1/2}$ was found in this stationary study. No rate coefficient has been

* Corresponding author.
E-mail address: cobos@inifta.unlp.edu.ar (C.J. Cobos).

http://dx.doi.org/10.1016/j.comptc.2016.05.015
2210-271X/

measured for reaction (4), and some conflictive and scattered values (from about 2×10^{-14} to 2×10^{-11} cm^3 molecule^{-1} s^{-1}) have been proposed for the SF_5-self association reaction [10,15,16]. However, the only available data for k_5 has been measured in liquid phase over the 153–233 K temperature range [17].

In the present study rate coefficient values have been calculated for reaction (4) using the transition state theory combined with relevant information of the potential energy surface provided by reliable density functional theory (DFT) formulations. Furthermore, the $k_4/k_5^{1/2}$ values of Ref. [14] have been employed to derive k_5. These rate coefficients were afterward compared with those resulting from statistical adiabatic channel model/classical trajectory (SACM/CT) calculations. In addition, for comparison with reaction (4), rate coefficients values for the similar reaction $SF_5 + Cl_2 \rightarrow SF_5Cl + Cl$ are also reported.

2. Computational methods

To obtain the molecular data relevant for the kinetics studies, the B3LYP [18–20], BMK [21], MPWB1K [22], BB1K [23] and M06-2X [24] formulations of the density functional were employed. The last four hybrid functionals have been specifically developed and validated for thermochemical kinetic studies as the present. They provide mean absolute deviations from well established experimental activation energies of 1.80 (BMK), 1.39 (MPWB1K), 1.40 (BB1K) and 1.32 kcal mol^{-1} (M06-2X)). These DFT approaches were combined with the Pople split-valence triple-ζ basis set 6-311+G(3df) [25]. Such extended basis set confers large radial and angular flexibility to represent electron density far from the nuclei and among the bonded atoms. The molecular structures were fully optimized via analytical gradient methods. For the estimation the harmonic vibration frequencies, analytical second order derivative methods were employed. The Synchronous Transit-Guided Quasi-Newton (STQN) method was employed for locating transition structures, which present only one imaginary frequency as confirmed by normal-mode analysis. Afterward, the transition states were verified by following the intrinsic reaction coordinate (IRC) from reactants to products. All calculations were carried out using the GAUSSIAN 09 suite of programs [26]. For the MPWB1K and BB1K methods, the BB95 and MPWB95 functionals with the "IOp" values of 3/76 = 0580004200 and 3/76 = 0560004400, as given by Truhlar and coworkers, were employed [22,23].

The calculation of the rate coefficients for the reactions of SF_5 with F_2 and Cl_2 was performed using the conventional transition state theory [27]. Limiting high pressure rate coefficients for the barrierless SF_5 self-association reaction were calculated with the SACM/CT [28] approach. For all cases the required molecular information was provided by either experimental studies or quantum-chemical calculations.

3. Molecular structures and harmonic vibrational frequencies

Equilibrium molecular structures estimated for SF_5 and S_2F_{10} with the B3LYP, BMK, MPWB1K, BB1K and M06-2X functionals together with the experimental values determined for S_2F_{10} by electron diffraction techniques [29] are listed in Table 1. The molecular geometries for SF_5 and S_2F_{10} are depicted in Fig. 1(a) and (b), respectively. A staggered configuration (dihedral angle D(FSSF) = 45°) of the SF_5 moieties was assumed in the analysis of the experimental data in Ref. [29]. Our calculations based on fully optimized structures support this D_{4d} symmetry. The measured equatorial S–F bond distances are 0.027 Å larger than the axial S–F′ bond distances. Values of 0.018, 0.013, 0.022, 0.022 and 0.014 Å are predicted for this difference for the B3LYP, BMK, BB1K, MPWB1K and M06-2X models. In addition, the experimental mean S–F bond distance of 1.569 Å can be compared with the values of 1.589, 1.565, 1.608, 1.607 and 1.569 Å, predicted by these DFT models. Overall, as Table 1 shows, the smallest differences between the theoretical and experimental S–F, S–F and S–S bond distances, −0.006, 0.008 and −0.002 Å, are provided by the BMK functional. However, reasonable bond distances are also predicted for the other employed models. In fact, the observed differences are, nearly, within the expected error limits [18–24]. The bond angles and dihedral angles are satisfactorily estimated by all DFT methods. Computed rotational constants calculated for SF_5 and S_2F_{10} using the molecular parameters of Table 1 are presented in Table 2.

Table 1
Structural parameters calculated for SF_5, S_2F_{10}, TS1 and SF_7 (bond lengths in Å, angles in degrees).

SF_5	B3LYP	BMK	BB1K	MPWB1K	M06-2X	Experimental
r(S–F)	1.623	1.595	1.647	1.646	1.595	
r(S–F′)	1.554	1.536	1.573	1.572	1.541	
∠(FSF)	89.9	90.0	89.9	89.9	90.0	
∠(FSF′)	91.8	91.3	91.8	91.8	91.3	
S_2F_{10}	B3LYP	BMK	BB1K	MPWB1K	M06-2X	Experimental[a]
r(S–F)	1.593	1.568	1.612	1.611	1.572	1.574
r(S–F″)	1.575	1.555	1.590	1.589	1.558	1.547
r(S–S)	2.327	2.272	2.337	2.332	2.249	2.274
∠(FSF)	90.0	90.0	90.0	90.0	90.0	
∠(FSF′)	89.8	89.8	90.1	90.1	89.8	89.8
∠(FSS)	90.2	90.2	89.9	89.9	90.2	
D(FSSF′)	45.0	45.1	44.7	44.9	45.0	
TS1	B3LYP	BMK	BB1K	MPWB1K	M06-2X	
r(S–F)	1.610	1.581	1.569	1.567	1.580	
r(S–F′)	1.552	1.534	1.526	1.524	1.538	
r(S–F″)	2.475	2.349	2.328	2.326	2.234	
r(F–F)	1.451	1.447	1.435	1.430	1.459	
∠(FSF′)	92.1	91.8	91.8	91.7	92.0	
∠(FSF″)	87.9	88.2	88.2	88.3	88.0	
SF_7	B3LYP	BMK	BB1K	MPWB1K	M06-2X	LSDA[b]
r(S–F)	1.577	1.555			1.558	1.567
r(S–F′)	1.577	1.555			1.558	1.565
r(S–F″)	1.580	1.558			1.562	1.584
r(F–F)	2.819	2.567			2.605	2.185
∠(FSF′)	90.1	90.1			90.1	90.4
∠(FSF″)	90.0	89.9			89.9	

[a] From Ref. [29].
[b] From Ref. [30].

The calculated SF_5 and S_2F_{10} harmonic vibrational frequencies together with the available experimental data are given in Table 3. A reasonable agreement between these sets of values is observed. Mean absolute deviations for the S_2F_{10} of 24, 36, 42, 41, and 33 cm^{-1} were found for the B3LYP, BMK, BB1K, MPWB1K and M06-2X models.

4. Rate coefficients for reactions $SF_5 + F_2 \rightarrow SF_6 + F$ and $SF_5 + Cl_2 \rightarrow SF_5Cl + Cl$

A single experimental study of reaction (4) has been reported [14]. This reaction participates in the gas-phase mechanism of the photochemical reaction between F_2 and SF_4. Although no complete kinetic information can be extracted for k_4 from these experiments, as above mentioned, the $k_4/k_5^{1/2}$ relationship has been determined at 213.3, 225.2 and 243.9 K. The activation energy obtained for this ratio is 4.0 kcal mol^{-1}. Considering reaction (5) is most likely barrierless (see below), such activation energy may be mostly attributed to reaction (4). To predict the Arrhenius parameters of this elementary process, TST calculations on relevant regions of the DFT potential energy surfaces were carried out. The

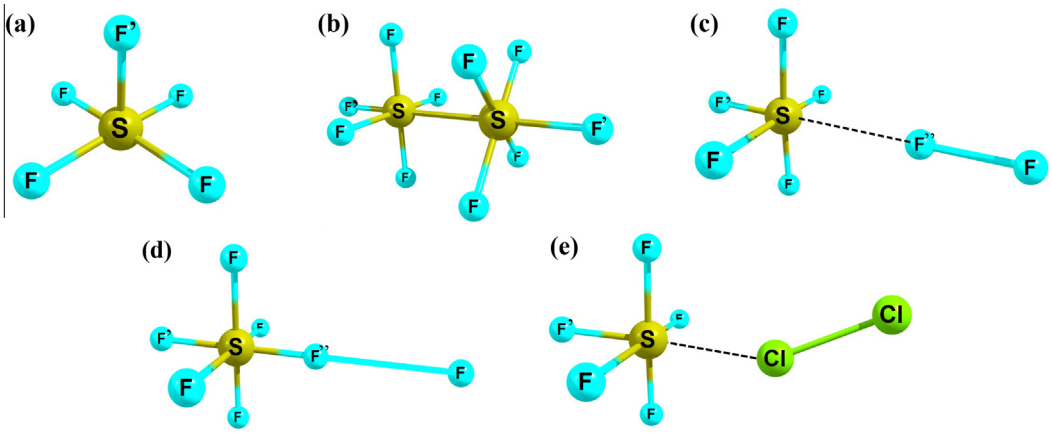

Fig. 1. Molecular Geometries obtained for SF_5 (a), S_2F_{10} (b), TS1 (c), SF_7 (d) and TS2 (e).

Table 2
Rotational constants (in cm^{-1}) calculated for SF_5, S_2F_{10} and TS1.

Rotational constants	SF_5			S_2F_{10}			TS1		
	A	*B*	*C*	*A*	*B*	*C*	*A*	*B*	*C*
B3LYP	0.120	0.120	0.084	0.044	0.022	0.022	0.086	0.034	0.034
BMK	0.124	0.124	0.087	0.045	0.023	0.023	0.089	0.036	0.036
BB1K	0.126	0.126	0.089	0.043	0.022	0.022	0.087	0.041	0.041
MPWB1K	0.116	0.116	0.082	0.043	0.022	0.022	0.090	0.037	0.037
M06-2X	0.124	0.124	0.087	0.045	0.023	0.023	0.089	0.038	0.038

resulting molecular parameters for the transition states (TS1) are listed in Table 1, while the structure is shown in Fig. 1(c). As it can be seen, the B3LYP functional leads to the largest S–F bond distance. The associated harmonic vibrational frequencies are given in Table 3. The derived B3LYP imaginary vibrational frequency of 160*i* cm^{-1} is notably smaller than those obtained with the other functionals, 454*i*–694*i* cm^{-1}.

The computed activation enthalpies $\Delta H_0^{\#}$ and enthalpy changes ΔH_0^0 for reaction (4) at 0 K are listed in Table 4. A schematic enthalpy diagram for this process is depicted in Fig. 2. As can be seen, significant differences between the B3LYP values and those obtained with the other selected functional were found. In fact, this functional predicts a barrier height 2–3 kcal mol^{-1} smaller than the calculated from the other functionals. However, even larger underestimations have been reported for other reactions [21]. The large difference observed in the ΔH_0^0 values, can be mostly attributed to errors in the calculated B3LYP/6-311+G(3df) total electronic energies for SF_5 and SF_6. The respective enthalpies of formation estimated at 0 K by total atomization energies of −194.0 and −267.7 kcal mol^{-1} are notably larger than those obtained, by instance, at the M06-2X/6-311+G(3df) level of −200.8 and −287.5 kcal mol^{-1}. These last values are in very good agreement with experimental, −200.0 kcal mol^{-1} [33], and CCSD(T)//B3LYP (with full extrapolated basis sets), −288.4 kcal mol^{-1} [34] consensus data for these species.

It is interesting to note that a very weak intermediate species SF_7 located between the transition state configuration and the SF_6 + F products is predicted by the employed B3LYP, BMK and M06-2X functionals. This species had been previously found using the local spin-density approximation (LSDA) [30]. The equilibrium SF_7 structure is depicted in Fig. 1(d) and the computed geometrical parameters are given in Table 1. The present calculations lead to F–F bond distances 0.4–0.6 Å larger than the estimated at the LSDA level. On the other hand, the resulting F_5SF–F bond strengths at the B3LYP, BMK and M06-2X levels are very small: 0.1, 0.1 and 0.5 kcal mol^{-1}. A much larger value of 3.5 kcal mol^{-1} is recovered by the LSDA calculations. In better agreement with the present calculations, the inclusion of non-local gradient corrections in the LSDA (LSDA/NL) leads to a bond dissociation energy of 1.2 kcal mol^{-1} [30].

The rate coefficients were calculated using the classical expression of the transition state theory $k = (k_BT/h)\ Q^{\#}/Q_AQ_B\ \exp(-\Delta H_0^{\#}/RT)$ [27]. Here, $Q^{\#}$, Q_A and Q_B are the total (electronic, translational, rotational and vibrational) partition functions for the transition state, the SF_5 and the F_2 molecules. The molecular input data of Tables 2–4 and the experimental values for the vibrational frequency and the rotational constant of F_2 [33] were employed for these calculations. The resulting individual k_4 values and its associated pre-exponential factors *A* and activation energies E_a are consigned in Table 5. Although the obtained Arrhenius parameters from the four functionals are in good agreement (the deviations in E_a values are smaller than the mean deviation of the employed models), due to the low temperatures investigated, large differences in the rate coefficients are observed. However, as to be discussed in Section 5, the experimental $k_4/k_5^{1/2}$ ratio provided a stringent key for select the more probable rate coefficients to reaction (4).

To compare the order of magnitude of k_4 estimated at 300 K, $\sim 1\times10^{-15}$–1×10^{-14} cm^3 $molecule^{-1}$ s^{-1}, the rate coefficients measured for similar reactions for the $FC(O)O_x$ (with x = 0–2) fluorine containing radicals were chosen [35–39]. The reported values for FCO + F_2 → FC(O)F + F, 4.5×10^{-14} cm^3 $molecule^{-1}$ s^{-1} [35], FC(O)O + F_2 → FC(O)OF + F, 3.4×10^{-15} cm^3 $molecule^{-1}$ s^{-1} [39], and FC(O)OO + F_2 → FC(O)OOF + F, $<1\times10^{-17}$ cm^3 $molecule^{-1}$ s^{-1} [39], show the ample range of rate coefficients that can be expected for the of this type of F atom abstraction processes.

For the sake of comparison, the Cl atom abstraction reaction from Cl_2 by the SF_5 radical,

$$SF_5 + Cl_2 \rightarrow SF_5Cl + Cl, \quad (8)$$

was also studied. To this end, the M06-2X6-311+G(3df) functional was selected. As reaction (4), this is also an activated process being the activation enthalpy at 0 K (TS2) of 6.2 kcal mol^{-1}. In addition, the derived reaction enthalpy of only −2.1 kcal mol^{-1} indicates that

Table 3
Harmonic vibrational frequencies (in cm^{-1}) calculated for SF_5, S_2F_{10} and TS1.

	SF_5	S_2F_{10}	TS1
B3LYP	226, 338, 338, 436, 494, 494, 522, 522, 601, 778, 778, 862	93, 171, 171, 223, 238, 238, 323, 326, 395, 395, 406, 406, 482, 482, 518, 547, 547, 556, 556, 597, 598, 610, 651, 660, 794, 830, 830, 889, 903, 903	160*i*, 64, 64, 133, 133, 234, 353, 354, 454, 479, 508, 508, 538, 570, 698, 806, 806, 865
BMK	247, 365, 365, 468, 536, 536, 569, 601, 657, 849, 849, 927	121, 205, 205, 273, 295, 295, 352, 376, 435, 435, 436, 436, 514, 514, 554, 584, 584, 594, 594, 649, 650, 662, 709, 731, 854, 903, 903, 968, 984, 984	454*i*, 70, 70, 167, 167, 261, 328, 384, 384, 488, 550, 550, 582, 620, 708, 885, 885, 933
BB1K	205, 312, 312, 402, 453, 453, 467, 517, 566, 732, 732, 815	188, 227, 231, 240, 274, 276, 351, 358, 408, 408, 410, 411, 479, 479, 500, 539, 539, 550, 550, 560, 560, 598, 620, 625, 765, 780, 780, 862, 862, 871	522*i*, 75, 75, 178, 187, 265, 326, 390, 390, 496, 559, 559, 588, 641, 723, 916, 916, 941
MPWB1K	207, 314, 314, 403, 454, 454, 471, 519, 568, 734, 734, 817	186, 234, 239, 251, 274, 279, 360, 360, 411, 411, 416, 416, 481, 481, 503, 541, 541, 553, 553, 561, 561, 602, 622, 627, 768, 782, 782, 864, 864, 876	520*i*, 76, 76, 178, 198, 267, 330, 392, 392, 498, 562, 562, 592, 646, 728, 922, 922, 947
M06-2X	245, 365, 365, 468, 535, 535, 566, 606, 606, 855, 855, 927	119, 202, 202, 270, 276, 276, 357, 361, 427, 427, 432, 432, 510, 510, 551, 578, 578, 589, 589, 647, 651, 657, 707, 726, 862, 902, 902, 971, 980, 980	694*i*, 90, 90, 211, 211, 262, 326, 388, 388, 492, 550, 550, 575, 629, 721, 902, 902, 934
Experimental	387, 387, 525, 525, 553, 633, 818, 818, 892[a]	115, 184.5, 184.5, 245.5, 247.5, 247.5, 414, 414, 427, 427, 507, 543.3, 573, 573, 590, 628, 628, 637.5, 683.5, 695, 824.5, 864.5, 864.5, 917, 937.8, 937.8[b]	

[a] From Ref. [31].
[b] From Ref. [32].

Table 4
Activation enthalpies and enthalpy changes (in kcal mol^{-1}) for reaction (4).

Level of theory	$\Delta H_0^{\#}$	ΔH_0^0
B3LYP	0.7	−57.4
BMK	2.6	−73.2
BB1K	3.5	−76.6
MPWB1K	2.8	−78.3
M06-2X	3.5	−73.3

this is a near thermoneutral process. In Fig. 2 a schematic enthalpy diagram of this process is presented. By contrast to the linear F_5S–F–F TS1 transition state, an angular F_5S–Cl–Cl configuration, as Fig. 1(e) shows, is predicted for TS2. Employing the above $\Delta H_0^{\#}$ value, the computed harmonic vibrational frequencies of 336*i*, 18, 72, 173, 187, 258, 298, 396, 398, 490, 558, 561, 571, 630, 674, 894, 899 and 902 cm^{-1} and the rotational constants $A = 0.086$, $B = 0.022$ and $C = 0.021$ cm^{-1} (derived from the $r(S–F)_{av} = 1.581$ Å, $r(S–F')$

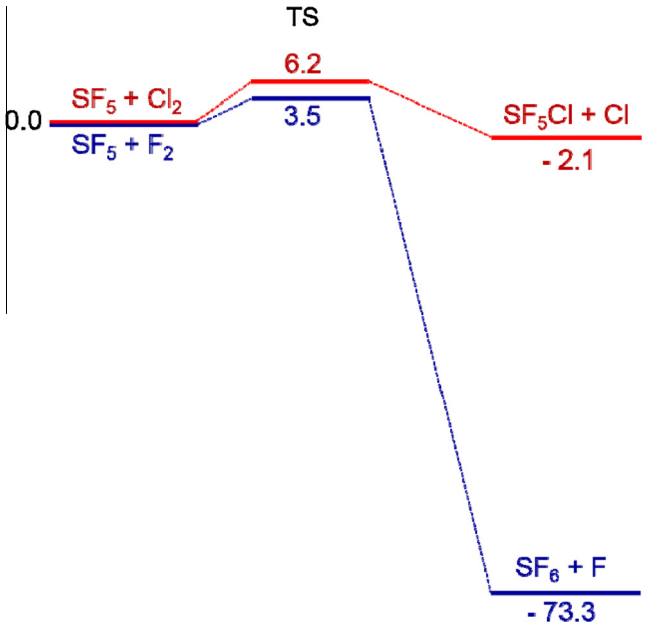

Fig. 2. Schematic enthalpy diagrams for reactions (4) and (8) calculated at the M06-2X/6-311+G(3df) level of theory.

Table 5
TST rate coefficients (in cm^3 $molecule^{-1}$ s^{-1}) and Arrhenius parameters A (in cm^3 $molecule^{-1}$ s^{-1}) and E_a (in kcal mol^{-1}) for reaction (4).

Level of theory	k_4			A	E_a
	$T = 213.3$ K	$T = 225.2$ K	$T = 243.9$ K		
BMK	1.3×10^{-15}	1.9×10^{-15}	3.3×10^{-15}	2.4×10^{-12}	3.2
BB1K	9.9×10^{-17}	1.7×10^{-16}	3.5×10^{-16}	2.0×10^{-12}	4.2
MPWB1K	6.6×10^{-16}	1.0×10^{-15}	1.8×10^{-15}	2.0×10^{-12}	3.4
M06-2X	7.4×10^{-17}	1.2×10^{-16}	2.4×10^{-16}	9.3×10^{-13}	4.0

= 1.547 Å, $r(S–Cl) = 2.353$ Å, $r(Cl–Cl) = 2.142$ Å and $\angle(SClCl) = 153.7°$ structural values, see Fig. 1(e)), the rate coefficients for reaction (8) were estimated. The resulting values at 298, 370, 430 and 500 K are 5.4×10^{-17}, 6.2×10^{-16}, 2.7×10^{-15} and 1.0×10^{-14} cm^3 $molecule^{-1}$ s^{-1}. These values can be reasonably represented by the Arrhenius expression $k_8 = 2.1 \times 10^{-11} \exp(-7.6 \text{ kcal mol}^{-1}/RT)$ cm^3 $molecule^{-1}$ s^{-1}. The predicted rate coefficient at 298 K for reaction (8) is about 20 times smaller than the calculated for reaction (4) at the same level of theory. To our knowledge, no experimental data for reaction (8) have been reported for comparison.

5. Rate coefficients for reaction $SF_5 + SF_5 \rightarrow S_2F_{10}$

DFT calculations performed along the minimum energy pathway of the SF_5 self-association (reaction (5)) at the B3LYP/6-311+G(3df) level revealed an energy profile without a maximum. This fact indicates the presence of a simple bond forming reaction exhibiting a smooth transition between the rotational modes of the SF_5 radicals and the S_2F_{10} transitional modes. These type of reactions are normally studied using the unimolecular reaction rate theory. In particular, an appropriate way to treat a reaction with such a potential at the high pressure limit is provided by the SACM/CT [28]. In this model the dynamics of a valence interaction between two linear rotors is calculated combining statistical adiabatic channel model (SACM) with classical trajectory (CT) calculations on a Morse potential. In the framework of the SACM, the high pressure rate coefficients can be factorized as $k_\infty = f_{rigid}\ k_\infty^{PST}$ [40], where k_∞^{PST} is the phase space theory rate coefficient

computed with the isotropic part of the potential, and f_{rigid} is the rigidity factor that accounts for dynamical constraints arising from the anisotropy of the potential energy surface. Following Ref. [40], k_∞^{PST} was obtained from the expression $k_\infty^{PST} = (k_B T/h)\,(h^2/2\pi\mu kT)^{3/2}\, f_{el}\, Q_{cent}$, where μ denotes the reduced mass of the collision pair for the A + B → C reaction, $f_{el} = Q_{el,C}/Q_{el,A}Q_{el,B}$ is the electronic degeneracy factor and $Q_{cent} = \Gamma(1 + 1/\nu)(k_B T/C_\nu)^{1/\nu}$ the centrifugal pseudo-partition function. Here, C_ν and ν are rotational parameters derived from the analysis of the centrifugal barriers [41]. For the present case, the values $C_\nu = 1.88 \times 10^{-3}$ cm^{-1} and $\nu = 1.12$ were employed.

For the calculation of the rigidity factor we treat the SF_5 radical as a quasi-linear rotor with the C_{4v} symmetry axis assimilated to a $C_{\infty v}$ axis of a linear rotor. The interaction between the two quasi-linear rotors is assumed to lead to the formation of a linear adduct. Under these conditions, the rigidity factor at 0 K was estimated as $f_{rigid}(T \to 0) = (1 + 1.5Z + Z^4)^{-1/4}$. Here, $Z = C_{eff}^2/2.34$ and $C_{eff} = \{[\varepsilon(r_e)]^2/2B_eD_e\}\,(kT/D_e)^{2\alpha/\beta-1}\,[1 + 0.42(2\alpha/\beta - 1) + (2\alpha/\beta - 1)^2]$. In the last expression $\varepsilon(r_e)$ is the geometrical average of the transitional frequencies at the equilibrium configuration (184.5 (2) and 247.5 (2) cm^{-1}, from Ref. [32]), B_e is the average of the largest rotational constants of the SF_5 radical (0.124 cm^{-1} (2) from B3LYP/6-311+G(3df) calculations) and $D_e \approx \Delta H_{298\,K}$ is the bond dissociation energy (47.3 kcal mol^{-1} [42]). To characterize the relevant potential energy features, a range parameter of $\beta = 1.9$ Å^{-1} was derived for the Morse potential using the S–S stretching frequency on S_2F_{10} (245.5 cm^{-1} [32]) while a standard anisotropy parameter of $\alpha/\beta = 0.5$, $\alpha = 0.93$ Å^{-1} (defined as $\omega = \omega_e \exp(-\alpha(r - r_e)$ [43]) was used to model the evolution of the transitional vibrational frequencies along the minimum energy path. Simplified SACM calculations show that a large number of experimental recombination/dissociation rate coefficients at the high pressure limit can be satisfactorily reproduced using a ratio $\alpha/\beta \approx 0.5 \pm 0.1$ [40,44–53]. The computed $f_{rigid}(T \to 0)$ values were afterward corrected by temperature dependencies: $f_{rigid}(T) = f_{rigid}(T \to 0)\,[1 - (2.31C_{eff})\,(\beta r_e)^{1/2}\exp(X/2.044)$ with $X = \ln(k_B T/D_e) - \beta r_e$, being $r_e = 2.4$ Å the distance between the center of mass of SF_5 radicals in S_2F_{10}. The resulting SACM/CT values at 213.3, 225.2 and 243.9 K are 8.4×10^{-13}, 8.3×10^{-13} and 8.1×10^{-13} cm^3 molecule^{-1} s^{-1}. Due to the large density of states of S_2F_{10}, no appreciable falloff effects can be expected for reaction (5), such that, at normal pressure conditions, $k_5 \approx k_{\infty,5}$.

No gas-phase experimental data are available for the SF_5 self-association. However, kinetic measurements have been performed by following the SF_5 concentrations by ESR after the photodissociation of SF_5Cl or SF_5OOSF_5 in nonpolar solvents (cyclopropane, and dichlorodifluoromethane) over the 153–233 K range [17]. On the basis of this data, the obtained equation $k_5 = 1.7 \times 10^{-11}\exp(-1.7$ kcal mol^{-1}/RT) cm^3 molecule^{-1} s^{-1} has been recommended for the gaseous phase reaction [54]. At 300 K, the SACM/CT calculations lead to a rate coefficient of 7.6×10^{-13} cm^3 molecule^{-1} s^{-1} while, in a good agreement, a value of 9.8×10^{-13} cm^3 molecule^{-1} s^{-1} is obtained from the kinetics data measured by Tait and Howard [17]. However, at lower temperatures, for instance at 200 K, a value of 8.6×10^{-13} cm^3 molecule^{-1} s^{-1} is obtained from the SACM/CT calculations and a rate coefficient a factor of 3 smaller, 2.4×10^{-13} cm^3 molecule^{-1} s^{-1}, is recovered from the above Arrhenius expression.

It appears interesting at this time to compare the above SACM/CT estimations with the k_5 values obtained combining the values derived from the $k_4/k_5^{1/2}$ expression with the TST rate coefficients derived for reaction (4) in Section 4. In Table 6 are listed the computed k_5 values using the k_4 values given in Table 4 and the $k_4/k_5^{1/2}$ values of 1.21, 1.99 and 3.94 M$^{-1/2}$ s$^{-1/2}$ determined at 213.3, 225.2 and 243.9 K [14]. It can be seen that BMK and the MPWB1K functional lead to very large k_5 values which are even larger than the calculated upper limit rate coefficients, $k_{5,\infty}^{PST} \approx 1 \times 10^{-10}$ cm^3 molecule^{-1} s^{-1}. Therefore, we have selected the average of the BB1K and M06-2X rate coefficients which leads to $k_4 = 1.4 \times 10^{-12}\exp(-4.1$ kcal mol^{-1}/RT) cm^3 molecule^{-1} s^{-1}.

Table 6
Rate coefficients for reaction (5) (in cm^3 molecule^{-1} s^{-1}) calculated combining the TST rate coefficients k_4 from Table 5 and the $k_4/k_5^{1/2}$ relationship (see text).

Level of theory	k_5		
	T = 213.3 K	T = 225.2 K	T = 243.9 K
BMK	6.6×10^{-10}	5.4×10^{-10}	4.1×10^{-10}
BB1K	4.1×10^{-12}	4.3×10^{-12}	4.6×10^{-12}
MPWB1K	1.8×10^{-10}	1.5×10^{-10}	1.3×10^{-10}
M06-2X	2.3×10^{-12}	2.3×10^{-12}	2.3×10^{-12}

Table 7
Rate coefficients for reaction (5) (in cm^3 molecule^{-1} s^{-1}).

T (K)	k_5[a]	$k_{5,\infty}^{PST}$[b]	f_{rigid}[b]	$k_{5,\infty}$[b]	k_5[c]
213.3	3.2×10^{-12}	9.7×10^{-11}	0.035	3.4×10^{-12}	3.1×10^{-13}
225.2	3.3×10^{-12}	9.9×10^{-11}	0.033	3.3×10^{-12}	3.8×10^{-13}
243.9	3.4×10^{-12}	1.0×10^{-10}	0.031	3.1×10^{-12}	5.1×10^{-13}

[a] From average TST calculations and the $k_4/k_5^{1/2}$ relationship (see text).
[b] SACM/CT calculations with $\alpha/\beta = 0.57$.
[c] From Refs. [17,54].

In Table 7 are listed the calculated rate coefficients. As can be seen, the k_5 values obtained with the relationship $k_4/k_5^{1/2}$ and the best TST predictions for k_4 are about a factor of 4 larger than the above SACM/CT estimations based on $\alpha/\beta = 0.5$. Nevertheless, as Table 7 shows, they can be well fitted increasing this parameter to 0.57, which is still within the expected range of $\alpha/\beta \approx 0.5 \pm 0.1$ [40,44–53]. By contrast, the rate coefficients recommended [55] on the basis of the liquid phase measurements of Ref. [17], are about 7–10 times smaller than those obtained here. It should be noted that the disproportionation reaction $SF_5 + SF_5 \to SF_4 + SF_6$ instead of the self-association reaction (5) might be predominant in these experiments [54]. Other k_5 values based on similar reactions or obtained from the analysis of complex reaction mechanisms have been reported at room temperature: 2×10^{-11} [15], 2×10^{-12} [16] and $<2 \times 10^{-14}$ cm^3 molecule^{-1} s^{-1} [10]. Our k_5 value of about 4×10^{-12} cm^3 molecule^{-1} s^{-1} at 300 K is closest to the value suggested by Benson and Bott [16]. The 50 times smaller upper limit proposed in Ref. [10] appears to be unreliable. Direct experimental measurements and/or theoretical kinetics studies of reaction (5) on ab initio characterized radial and angular parts of the potential energy surface, similar to those recently performed for other reactions [55–57], are clearly desirable.

6. Conclusions

The present quantum–mechanical and kinetic study of the gas phase reactions of SF_5 with F_2 and Cl_2 provides TST rate coefficients $k_4 = 1.4 \times 10^{-12}\exp(-4.1$ kcal mol^{-1}/RT) and $k_8 = 2.1 \times 10^{-11}\exp(-7.6$ kcal mol^{-1}/RT) cm^3 molecule^{-1} s^{-1} for these atom abstraction elemental processes. Combining the k_4 values with the experimentally determined ratio $k_4/k_5^{1/2}$ at 213–244 K [14], rate coefficients were derived for the self-SF_5 association reaction (5). The extrapolated room temperature value for k_5 of about 4×10^{-12} cm^3 molecule^{-1} s^{-1} is consistent with the value estimated by Benson and Bott [16] and disagrees strongly with a proposed upper limit [10]. In addition, the results are consistent with those predicted by standard SACM/CT calculations.

Acknowledgements

This research project was supported by the Universidad Antonio Nariño (Project No. 20141084), the Universidad Nacional de La

Plata (11/X676), the Consejo Nacional de InvestigacionesCientíficas y Técnicas CONICET (PIP-615, PIP-1134) and the Agencia Nacional de Promoción Científica y Tecnológica (PICT-478).

Appendix A. Supplementary material

Supplementary data associated with this article can be found, in the online version, at http://dx.doi.org/10.1016/j.comptc.2016.05.015.

References

[1] R.A. Morrow, Survey of the electron and ion transport properties of SF_6, IEEE Trans. Plasma Sci. 14 (1986) 234–239.
[2] L.G. Christophorou, J.K. Olthoff, R.J. Van Brunt, Sulfur hexafluoride and the electric power industry, IEEE Electr. Insul. Mag. 13 (1997) 20–24.
[3] M. Maiss, C.A. Brenninkmeijer, Atmospheric SF_6: trends, sources, and prospects, Environ. Sci. Technol. 32 (1998) 3077–3086.
[4] H. Kitabayashi, H. Fujii, T. Ooishi, Charging of glass substrate by plasma exposure, Jpn. J. Appl. Phys. 38 (1999) 2964–2968.
[5] J.T. Herron, Fundamental processes of SF_6 decomposition and oxidation in glow and corona discharges, IEEE Trans. Electr. Insul. 25 (1990) 75–94.
[6] C.-H. Liu, S. Palanisamy, S.-M. Chen, P.-S. Wu, L. Yao, B.-S. Lou, Mechanism of formation of SF_6 decomposition gas products and its identification by GC–MS and electrochemical methods: a mini review, Int. J. Electrochem. Sci. 10 (2015) 4223–4231.
[7] W.T. Sturges, T.J. Wallington, M.D. Hurley, K.P. Shine, K. Sihra, A. Engel, D.E. Oram, S.A. Penkett, R. Mulvaney, C.A.M. Brenninkmeijer, A potent greenhouse gas identified in the atmosphere: SF_5CF_3, Science 289 (2000) 611–613.
[8] J. Czarnowski, H.J. Schumacher, Kinetics of the thermal decomposition of bis-pentafluorine sulfur peroxide in the presence of carbon monoxide, Int. J. Chem. Kinet. 9 (1978) 111–116.
[9] J. Czarnowski, H.J. Schumacher, The kinetics and the mechanism of the thermal decomposition of bis-pentafluorosulfurtrioxide ($F_5SOOOSF_5$), Int. J. Chem. Kinet. 11 (1979) 613–619.
[10] J. Czarnowski, H.J. Schumacher, The kinetics and the thermal decomposition of bis-pentafluorosulfur trioxide ($F_5SOOOSF_5$) in the presence of carbon monoxide, Int. J. Chem. Kinet. 11 (1979) 1089–1096.
[11] M. Feliz, H.J. Schumacher, Die Kinetik der durch SF_5O radikale sensibilisierten CO-oxydation, J. Photochem. 15 (1981) 109–118.
[12] A.C. González, H.J. Schumacher, Die kinetik der thermischen reaktion zwischen schwefeltetrafluorid und fluor in gegenwart von sauerstoff, Z. Phys. Chem. NF 127 (1981) 167–177.
[13] A.C. González, H.J. Schumacher, Die kinetik und der mechanismus der photochemischen reaktion zwischen F_2O und SF_4 bei 265 nm, Z. Phys. Chem. NF 20 (1982) 85–99.
[14] P.F. Aramendía, H.J. Schumacher, The kinetics and mechanism of the photochemical reaction between SF_4 and fluorine at 365 nm, Z. Phys. Chem. NF 28 (1985) 491–502.
[15] H.W. Sidebottom, J.M. Tedder, J.C. Walton, Free radical addition to olefins. Part 4. The light-induced addition of sulphur chloride pentafluoride to ethylene, Trans. Faraday Soc. 65 (1969) 2103–2109.
[16] S.W. Benson, J. Bott, The kinetics and thermochemistry of S_2F_{10} pyrolysis, Int. J. Chem. Kinet. 1 (1969) 451–458.
[17] J.C. Tait, J.A. Howard, An electron spin resonance study of some reactions of pentafluorosulfuranyl (SF_5), Can. J. Chem. 53 (1975) 2361–2364.
[18] A.D. Becke, Density-functional exchange-energy approximation with correct asymptotic behavior, Phys. Rev. A 38 (1988) 3098–3100.
[19] A.D. Becke, Density-functional thermochemistry. III. The role of exact exchange, J. Chem. Phys. 98 (1993) 5648–5652.
[20] C. Lee, W. Yang, R.G. Parr, Development of the Colle-Salvetti correlation-energy formula into a functional of the electron density, Phys. Rev. B 37 (1988) 785–789.
[21] A.D. Boese, J.M.L. Martin, Development of density functionals for thermochemical kinetics, J. Chem. Phys. 121 (2004) 3405–3416.
[22] Y. Zhao, D.G. Truhlar, Hybrid meta density functional theory methods for thermochemistry, thermochemical kinetics, and noncovalent interactions: the MPW1B95 and MPWB1K models and comparative assessments for hydrogen bonding and van der Waals interactions, J. Phys. Chem. A 108 (2004) 6908–6918.
[23] Y. Zhao, B.J. Lynch, D.G. Truhlar, Development and assessment of a new hybrid density functional model for thermochemical kinetics, J. Phys. Chem. A 108 (2004) 2715–2719.
[24] Y. Zhao, D.G. Truhlar, The M06 suite of density functionals for main group thermochemistry, thermochemical kinetics, noncovalent interactions, excited states, and transition elements: two new functionals and systematic testing of four M06-class functionals and 12 other functionals, Theor. Chem. Acc. 120 (2008) 215–241.
[25] M.J. Frisch, J.A. Pople, J.S. Binkley, Self-consistent molecular orbital methods 25. Supplementary functions for Gaussian basis sets, J. Chem. Phys. 80 (1984) 3265–3269 (and references therein).
[26] M.J. Frisch, et al., Gaussian Inc., Revision A.02, Wallingford, CT, USA, 2009.
[27] S. Glasstone, K.J. Laidler, H. Eyring, The Theory of Rate Processes: The Kinetics of Chemical Reactions, Viscosity, Diffusion and Electrochemical Phenomena, McGraw-Hill Book Company Inc., New York, 1941.
[28] A.I. Maergoiz, E.E. Nikitin, J. Troe, V.G. Ushakov, Classical trajectory and statistical adiabatic channel study of the dynamics of capture and unimolecular bond fission. V. Valence interactions between two linear rotors, J. Chem. Phys. 108 (1998) 9987–9998.
[29] H. Oberhammer, O. Lösking, H. Willner, A re-investigation of the gas-phase structure of disulfur decafluoride S_2F_{10}, J. Mol. Struct. 192 (1989) 171–175.
[30] G.L. Gutsev, Superhalogens among sp-elements: SF_7 184 (1991) 91–98.
[31] M. Kronberg, S. von Ahsen, H. Willner, J.S. Francisco, The SF_5O_x radicals, $x = 0$–3, Angew. Chem. Int. Ed. 44 (2005) 253–257.
[32] L.H. Jones, S.A. Ekberg, Vibrational spectrum and potential constants for S_2F_{10}, Spectrochim. Acta 36A (1980) 761–767.
[33] M.W. Chase, NIST-JANAF thermochemical tables, J. Phys. Chem. Ref. Data, Monogr. No. 9 (1998).
[34] C.W. Bauschlicher, A. Ricca, Accurate heats of formation for SF_n, SF_n^+, and SF_n^- for $n = 1$–6, J. Phys. Chem. A 102 (1998) 4722–4727.
[35] M.M. Maricq, J.J. Szente, G.A. Khitrov, J.S. Francisco, FCO: UV spectrum, self-reaction kinetics and chain reaction with F_2, Chem. Phys. Lett. 199 (1992) 71–77.
[36] M.M. Maricq, J.J. Szente, Z. Li, J.S. Francisco, Visible absorption spectroscopy of the B $^2A_1$–X $^2B_2$ transition of fluoroformyloxyl radical, FC(O)O, J. Chem. Phys. 98 (1993) 784–790.
[37] M.M. Maricq, J.J. Szente, T.S. Dibble, J.S. Francisco, Atmospheric chemical kinetics of FC(O)O, J. Phys. Chem. 98 (1994) 12294–12309.
[38] J.S. Francisco, M.M. Maricq, Making sure that hydrofluorocarbons are "ozone friendly", Acc. Chem. Res. 29 (1996) 391–397.
[39] M.P. Badenes, E. Castellano, C.J. Cobos, A.E. Croce, M.E. Tucceri, Kinetics of the reactions of $FC(O)O_2$ radicals with F atoms and F_2, Chem. Phys. 253 (2000) 205–217.
[40] C.J. Cobos, J. Troe, Theory of thermal unimolecular reactions at high pressures. II. Analysis of experimental results, J. Chem. Phys. 83 (1985) 1010–1015.
[41] J. Troe, Theory of thermal unimolecular reactions at high pressures, J. Chem. Phys. 75 (1981) 226–237.
[42] K.K. Irikura, Thermochemistry of disulfur decafluoride, S_2F_{10}, J. Chem. Phys. 103 (1995) 10162–10168.
[43] M. Quack, J. Troe, Specific rate constants of unimolecular processes, Ber. Bunsenges. Phys. Chem. 78 (1974) 240–252.
[44] C.J. Cobos, A.E. Croce, H. Hippler, E. Castellano, Direct determination of the limiting high pressure rate constants of the system $FSO_3 + FSO_3 \Longleftrightarrow F_2S_2O_6$ over the temperature range 293–381 K, J. Phys. Chem. 93 (1989) 3089–3094.
[45] C.J. Cobos, A.E. Croce, E. Castellano, Kinetics of the recombination reaction between F atoms and FCO radicals, Chem. Phys. Lett. 239 (1995) 320–325.
[46] A.E. Croce, C.J. Cobos, E. Castellano, Experimental and theoretical study of the recombination reaction of FC(O)O radicals, Chem. Phys. 211 (1996) 215–226.
[47] M.P. Badenes, E. Castellano, C.J. Cobos, A.E. Croce, M.E. Tucceri, Rate coefficient for the reaction $FCO + FC(O)O_2 \rightarrow 2\ FC(O)O$ at 296 K, Chem. Phys. Lett. 303 (1999) 482–488.
[48] M.P. Badenes, A.E. Croce, C.J. Cobos, Experimental and theoretical study of the recombination reaction $F + FC(O)O + M \rightarrow FC(O)OF + M$, Phys. Chem. Chem. Phys. 6 (2004) 747–755.
[49] M.E. Tucceri, A.E. Croce, C.J. Cobos, Limiting high-pressure rate coefficient for the recombination reaction $FSO_2 + FSO_3 \rightarrow FS(O_2)O(O_2)SF$: an experimental and theoretical study, Chem. Phys. Lett. 404 (2005) 232–236.
[50] C.J. Cobos, A.E. Croce, K. Luther, J. Troe, Temperature and pressure dependence of the reaction $2\ CF_3\ (+M) \rightarrow C_2F_6\ (+M)$, J. Phys. Chem. A 114 (2010) 4747–4754.
[51] C.J. Cobos, A.E. Croce, K. Luther, J. Troe, Shock wave study of the thermal decomposition of CF_3 and CF_2 radicals, J. Phys. Chem. A 114 (2010) 4755–4761.
[52] C. Buendía-Atencio, C.J. Cobos, Theoretical study of the thermochemistry and the kinetics of the SF_xCl ($x = 0$ to 5) series, J. Fluorine Chem. 132 (2011) 474–481.
[53] M.P. Badenes, M.E. Tucceri, C.J. Cobos, Formation and dissociation kinetics of the $FC(O)OOO(O)CF$, $FS(O_2)OOO(O_2)SF$ and $FC(O)OOO(O_2)SF$ trioxides. A theoretical study, Chem. Phys. Lett. 616–617 (2014) 81–85.
[54] J.T. Herron, A critical review of the chemical kinetics of SF_4, SF_5, and S_2F_{10} in the gas phase, Int. J. Chem. Kinet. 19 (1987) 129–142.
[55] C.J. Cobos, A.E. Croce, K. Luther, L. Soelter, E. Tellbach, J. Troe, Experimental and modeling study of the reaction $C_2F_4\ (+M) \leftrightarrow CF_2 + CF_2\ (+M)$, J. Phys. Chem. A 117 (2013) 11420–11429.
[56] Adela E. Croce, Carlos J. Cobos, Theoretical kinetics study of the reactions forming the ClCO radical cycle in the middle atmosphere of Venus, Z. Phys. Chem. 229 (2015) 1541–1559.
[57] M.E. Tucceri, M.P. Badenes, L.L.B. Bracco, C.J. Cobos, Thermal decomposition of 3-bromopropene. A theoretical kinetic investigation, J. Phys. Chem. A 120 (2016) 2285–2294.